Solid Solution $(Li_{1.3-y}Cu_y)V_3O_8$: Structure and Electrochemistry

P. Rozier,*,† M. Morcrette,‡ P. Martin,‡ L. Laffont,‡ and J-M. Tarascon‡

CEMES, CNRS, BP 94347, 31055 Toulouse Cedex, France, and LRCS, Université de Picardie Jules Verne, 33 rue Saint-Leu, 80039 Amiens, France

Received September 2, 2004. Revised Manuscript Received December 10, 2004

Members of the $(Li_{1.3-y}Cu_y)V_3O_8$ solid solution were synthesized for $0 < y < 1$ by annealing, in evacuated sealed quartz ampules, stoichiometric mixtures of $LiVO_3$, Cu_2O, and V_2O_5, and their electrochemical performance in $(Li_{1.3-y}Cu_y)V_3O_8$/Li cells was studied as a function of *y*. The rationale for carrying out such a synthesis in a vacuum rather than in air, as commonly practiced, is given, and the origin of the Cu solid solution limit is explained on the basis of structural considerations. With the exception of the rate capability, the electrochemical performances of the $(Li_{1.3-y}Cu_y)V_3O_8$ samples both in terms of capacity and capacity retention decreased with increasing *y*. The decrease in reversibility of the Li insertion/deinsertion process with increasing *y* is shown, through *in situ* X-rays and HRTEM measurements, to be nested in the partial reversibility of the Cu extrusion/re-injection process on cycling.

Introduction

In 1957 while studying the $Li_2O-V_2O_5$ system, Wadsley et al. succeeded in growing a single crystal of a new phase by heat-treating a 1:2 ratio of Li_2CO_3 and V_2O_5. This new phase was identified as $\gamma Li_{1+x}V_3O_8$.[1] Twenty years later, $Li_{1+x}V_3O_8$ was proposed as an alternative to V_6O_{13} cathode material in secondary lithium cells.[2] Since then, numerous studies have been reported showing the dependence of the electrochemical performance of $Li_{1+x}V_3O_8$ as a function of its synthesis method[3−9] and, therefore, of its texture and morphology. Following a different path and inspired by Thackeray's work[10] on intermetallic negative electrode materials (Cu_2Sb, InSb) dealing with displacement reactions, we re-investigated the Cu−V−O system, and recently reported a new copper vanadate, $Cu_{2.33}V_4O_{11}$,[11,12] which shows an unusual electrochemical reactivity toward Li, i.e., it can reversibly react with 6 Li per formula unit, even though its structure contains no vacant sites to host Li. Through combined X-ray and microscopy studies we deduced that discharge/charge cycles involved repeated extrusion and re-injection of copper within the host structure as well as insertion/de-insertion of Li. Such a peculiar behavior was ascribed to both the presence of highly mobile copper ions and the host network flexibility. Schematically, the $[V_4O_{11}]$ layers are built up with $[V_4O_{12}]$ chains sharing an oxygen that acts as a pivot allowing the puckering of the layers. In contrast, the $Li_{1.3}V_3O_8$ electrode reaction with Li is a classical insertion/de-insertion process, and the $Li_{1.3}V_3O_8$ host network appears more flexible than that of $Cu_{2.33}V_4O_{11}$. $[V_3O_8]$ layers are built up with the same $[V_4O_{12}]$ chains but connected to each other via a $[VO_3]$ string built up with edge-sharing VO_5 square pyramids. This $[VO_3]$ string shares one oxygen with each of the $[V_4O_{12}]$ ones, and acts as a hinge allowing an enhanced puckering of the resulting $[V_3O_8]$ layers. Hence, our desire to investigate the possibility of synthesizing a pure $Cu_{1+x}V_3O_8$ compound, and study its electrochemical behavior. Such attempts at outlining both inserted cations as well as network flexibility influence on the electrochemical behavior are described within the manuscript. Even though we did not succeed in synthesizing a fully substituted $Li_{1.3-y}Cu_yV_3O_8$ phase, the study provides a possible explanation for the importance of the synthesis method on the performance of $Li_{1.3}V_3O_8$, and clarifies the role of copper on $Li_{1.3-y}Cu_yV_3O_8$ structure and electrochemical behavior.

Experimental Section

Synthesis. Samples of the $Li_{1.3-y}Cu_yV_3O_8$ phase were prepared following the chemical reaction

$$(1.3-y)\,LiVO_3 + \left(\frac{y}{2}\right)Cu_2O + \frac{(1.4+y)}{2}\,V_2O_5 + 0.3VO_2 \rightarrow Li_{1.3-y}Cu_yV_{2.7}^{5+}V_{0.3}^{4+}O_8$$

In each case, the same protocol was followed. Appropriate amounts of reactants were mixed together in an agate mortar. The resulting mixture was placed in a quartz tube sealed under vacuum and heat-treated at 500 °C during 48 h. After the mixture was ground, a second heat treatment was applied under the same conditions to ensure a better crystallinity. $LiVO_3$ was synthesized by heat-treating

* To whom correspondence should be addressed. E-mail: rozier@cemes.fr.
† CEMES, CNRS.
‡ LRCS, Université de Picardie Jules Verne.

(1) Wadsley, A. D. *Acta Crystallogr.* **1957**, *10*, 261.
(2) Besenhard, J. O.; Schöllhorn, R. *J. Power Sources* **1976**, *1*, 267.
(3) Friberg, S.; Roberts, K.; Lindner, G.; Nyberg, K., Eds. *Environnemental Engineering*; Reidel: Dordrecht, The Netherlands, 1973.
(4) Eriksson, L.; Alm, B. *Water Sci. Technol.* **1993**, *28*, 203.
(5) Nayak, P. L.; Lenke, S. J. *J. Macromol. Sci. Chem. A* **1980**, *19*, 83.
(6) Renders, G.; Broze, G.; Jerome, R.; Teyssie, Ph. J. *Macromol. Sci. Chem. A* **1981**, *16*, 1399.
(7) Fernandez, M. D.; Guzman, G. M. *J. Polym. Sci.* **1989**, *Part A-1 27*, 3703.
(8) Kumagai, N.; Yu, A. *J. Electrochem. Soc.* **1997**, *144*, 830.
(9) Kawakita, J.; Kato, T.; Katoyama, Y.; Miura, T.; Kishi, T. *J. Power Sources* **1999**, *448*, 81−82.
(10) Fransson, L. M. L.; Vaughey, J. T.; Benedek, R.; Edstrôm, K.; Thomas, J. O.; Thackeray, M. M. *Electrochem. Commun.* **2001**, *3*, 317−323.
(11) Rozier, P.; Satto, C.; Galy, J. *Solid State Sci.* **2000**, *2*, 595.
(12) Morcrette, M.; Rozier, P.; Dupont, L.; Mugnier, E.; Sannier, L.; Galy, J.; Tarascon, J. M. *Nat. Mater.* **2003**, *2*, 755.

10.1021/cm048518f CCC: $30.25
Published on Web 02/04/2005

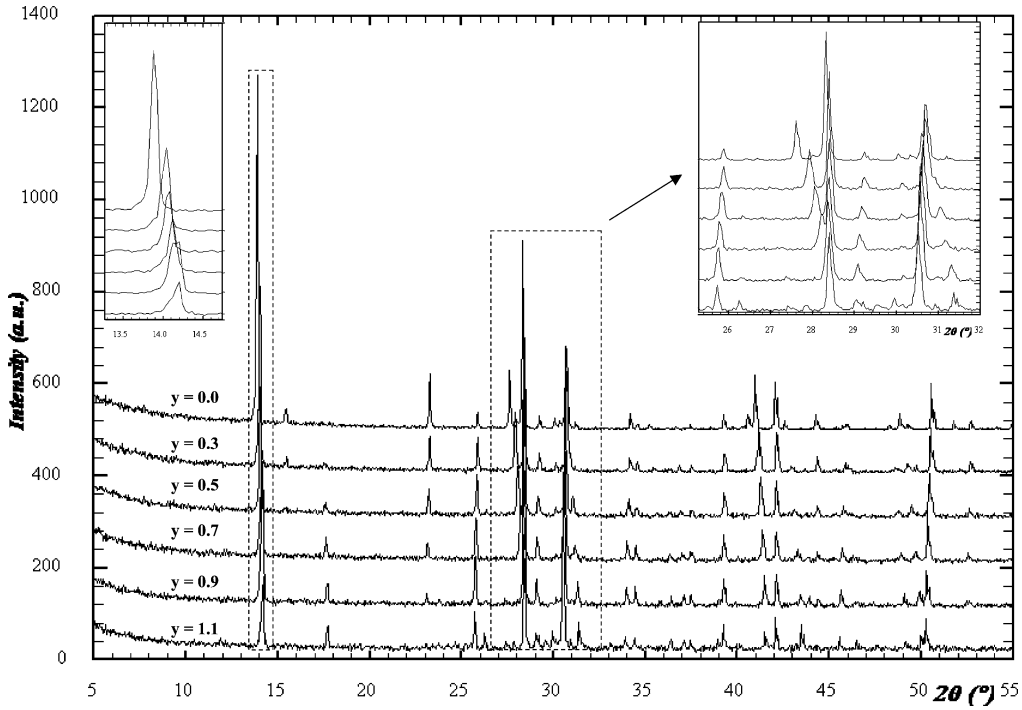

Figure 1. XRD pattern of the $Li_{1.3-y}Cu_yV_3O_8$ solid solution.

a stoichiometric mixture of Li_2CO_3 and V_2O_5 powders at 600 °C for 12 h. VO_2 was prepared from V_2O_5 and V_2O_3 powders mixed together and heated at 630 °C under vacuum for 12 h. V_2O_3 was previously obtained by reduction, under hydrogen, of V_2O_5 in two steps: 4 h at 500 °C followed by 4 h at 800 °C to complete the reduction process and ensure sample homogeneity.

XRD, SEM, TEM Characterization. Samples were analyzed by X-ray diffraction. The patterns were collected with Cu Kα radiation using a Seifert XRD 3000 TT diffractometer equipped with a back graphite monochromator. Electrochemical *in situ* experiments were examined by a Scintag diffractometer operating in Bragg−Brentano geometry with Cu Kα radiation. The morphology and composition of the powders were investigated by scanning electron microscopy (SEM) with a Philips XL 30 field emission gun (FEG), coupled to an Oxford Link instrument for energy-dispersive X-ray spectroscopy (EDS). Our HRTEM investigations on the chemically/electrochemically oxidized/reduced Cu−V−O samples were conducted on a Tecnai F20 ST transmission electron microscope, equipped with both EDS analysis capabilities and a home-designed sample holder for moisture sensitive samples.

Electrochemical Tests. If not otherwise specified, the materials were tested in standard 2035-size coin cells using (1) a plastic positive electrode disk containing 64 wt % of $Li_{1.3-y}Cu_yV_3O_8$ materials, 8 wt % SP carbon black (MMM Carbon, Belgium), and 28 wt % PVDF−HFP copolymer binder (the electrode films were cast and processed using a previously reported procedure[13]), (2) a 1-cm^2 disk of Li foil as the negative electrode member, and (3) a Whatman GF/D borosilicate glass fiber sheet separator saturated with a 1 M $LiPF_6$ electrolyte solution in a 1:1 (by weight) dimethyl carbonate/ethylene carbonate. The cells were assembled in an argon-filled glovebox at a dewpoint of 80 °C. The lithium reactivity was monitored with a "VMP" potentiostat/galvanostat (Biologic SA, Claix, France), operating in both galvanostatic and potentiostatic modes. *In situ* X-ray diffraction electrochemical cells assembled similarly to our Swagelok cell,[14] but having a beryllium window as current collector on the positive side, were placed on the same Scintag diffractometer as above, and also connected to the Mac-Pile system for successive charge/discharge cycles.

Throughout the paper, *C*/*n* is defined as the theoretical capacity over *n* hours. This theoretical capacity is equal to 380 mAh/g for $Li_{1.3}V_3O_8$ (4 lithiums) and 320 mAh/g for $Li_{0.4}Cu_{0.9}V_3O_8$, if one supposes that the same amount of lithium can react with this last compound.

Results

(a) Chemical Studies of the $Li_{1.3-y}Cu_yV_3O_8$ Solid Solution. Syntheses were made for *y* values ranging from 0 to 1.3. Examination of the X-ray powder patterns (XRPD) of the resulting samples shows only the presence of single-phased materials for $y < 1$ (Figure 1). With higher Cu content, indexing of the XRPD patterns enables the identification of the member with the highest copper content in the $Li_{1.3-y}Cu_yV_3O_8$ solid solution (namely the composition $Li_{0.4}Cu_{0.9}V_3O_8$) mixed with known copper vanadates such as CuV_2O_6, and $\beta Cu_xV_2O_5$, which is the main phase (Figure 2) for the composition "$Cu_{1.3}V_3O_8$".

The Bragg peaks of single-phased products XRPD were indexed by comparison with those calculated from $Li_{1.3}V_3O_8$ structural data. The cell parameters were refined by the least-squares method. The results are reported Table 1. Examination of these results shows that with increasing copper content the **a** cell parameter and β angle decrease while the **b** and **c** cell parameters remain almost constant within the accuracy of the experiment.

Considering the reactants used for the synthesis (Cu^{1+} as in Cu_2O), the expected charge repartition within the final compounds should be $Li_{1.3-y}Cu_y^{1+}V_{2.7}^{5+}V_{0.3}^{4+}O_8$. Therefore,

(13) Orsini, F.; Du Pasquier, A.; Beaudouin, B.; Tarascon, J. M.; Trentin, M.; Langenhuizen, N.; De Beer, E.; Notten, P. *J. Power Sources* **1999**, *81*−*82*, 918−921.

(14) Morcrette, M.; Chabre, Y.; Vaughan, G.; Amatucci, G.; Leriche, J−B.; Patoux, S.; Masquelier, C.; Tarascon, J−M. *Electrochem. Acta* **2002**, *47*, 3137−3149.

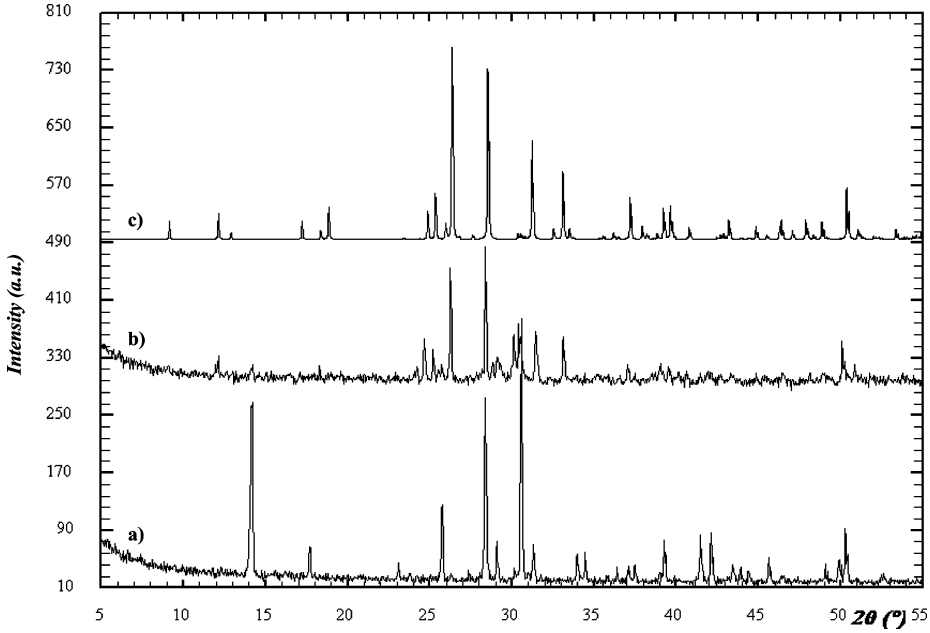

Figure 2. Comparison between XRD patterns: experimental for (a) $Li_{0.4}Cu_{0.9}V_3O_8$ and (b) "$Li_{0.1}Cu_{1.2}V_3O_8$", and calculated for (c) $\beta Cu_xV_2O_5$.

Table 1. Cell Parameters Evolution versus Copper Content in the Solid Solution $Li_{1.3-y}Cu_yV_3O_8$

y	a (Å)	b (Å)	c (Å)	β (deg)	V (Å^3)
0.0	6.677	3.600	12.030	107.66	275.5
0.3	6.611	3.609	12.005	107.26	273.5
0.5	6.574	3.613	12.017	107.01	272.9
0.7	6.540	3.620	12.033	106.78	272.7
0.9	6.514	3.624	12.034	106.59	272.3
1.1	6.503	3.628	12.036	106.41	272.4

we cannot rule out the feasibility of an internal oxydo-reduction process according to the equation $Cu^{1+} + V^{5+} \rightarrow Cu^{2+} + V^{4+}$. To check such a hypothesis, the Curie constant for each sample was measured, using the classic Faraday method. For $y = 0$, a Curie constant of 0.108/M is measured in good agreement with the theoretical value of 0.113 ($C = n(n + 2)/8*0.3$) that is expected for $0.3V^{4+}$ per formula unit. This value barely changes with increasing y suggesting that internal oxydo-reductive process between Cu^{1+} and V^{5+}, which would generate magnetic Cu^{2+} ions, does not occur. This was further confirmed by EPR measurements that show only a single line associated with V^{4+}.

(b) Electrochemistry. To determine the influence of copper, the electrochemical behavior of the different members of the solid solution were studied. For the sake of conciseness, we report only results for the end members $Li_{1.3}V_3O_8$ and $Li_{0.4}Cu_{0.9}V_3O_8$. Coin cells using about 10 mg of either $Li_{1.3}V_3O_8$ or $Li_{0.4}Cu_{0.9}V_3O_8$ as the positive electrode and Li metal as the negative electrode were cycled between 3.5 and 1.5 V at a C/10 rate (e.g., the full theoretical capacity in 10 h).

Kinetic limitations of $Li_{1.3}V_3O_8$ are often encountered in the literature. With classical manual carbon mixing, we experienced difficulties in achieving capacities greater than 230 mAh/g at C/10 (Figure 3a), while the theoretical value is about 380 mAh/g. As an attempt to tap more of the theoretical capacity, we implemented our recent experience with the poorly conducting $LiFePO_4$ insertion compound, which has shown the feasibility to fully use the capacity of

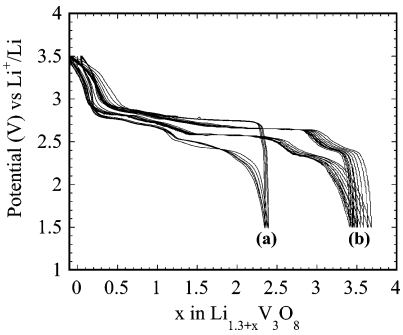

Figure 3. Potential versus composition curve of a $Li_{1.3}V_3O_8$| Li cell with (b) and without (a) 30-min ball milling of the carbon/active material electrode.

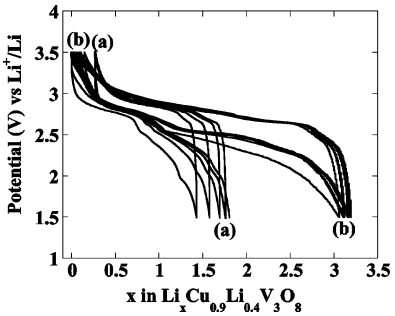

Figure 4. Potential versus composition curve of a $Li_{0.4}Cu_{0.9}V_3O_8$| Li cell with (b) and without (a) 30-min ball milling of the carbon/active material electrode.

this material, by preparing carbon/$LiFePO_4$ composites by shock ball-milling.[15] In this procedure, 200 mg of LiV_3O_8 mixed with 40 mg of C were placed in a stainless steel container with one stainless steel ball (6.5 g) so that the ratio was 27. The samples were then placed in a ball mixer for about 30 min, a time that proved to give the best electrochemical results. Using this simple way of preparation, $Li_{1.3}V_3O_8$/C composite electrodes capable of reversibly

(15) Morcrette, M.; Wurm, C.; Masquelier, C. *Solid State Sci.* **2002**, *14*, 1166−1173.

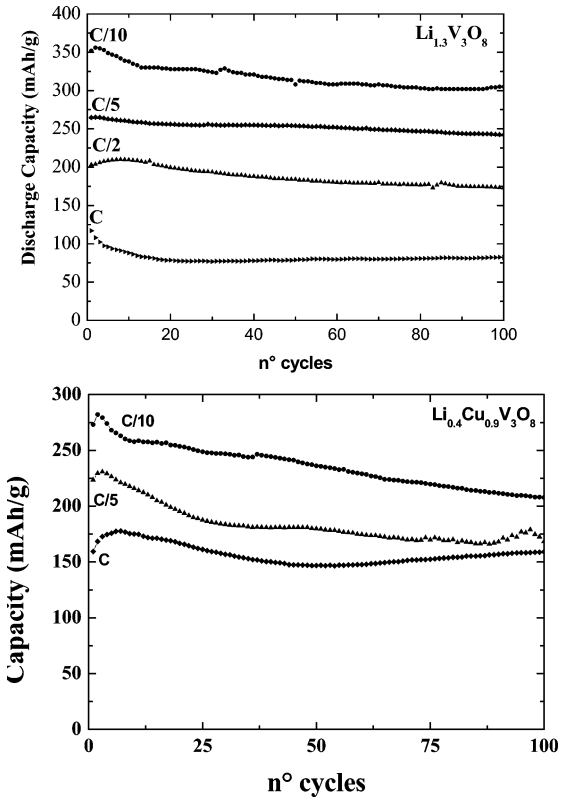

Figure 5. (a) Capacity retention (values recorded in discharge) as a function of the number of cycles at different rates (C/10, C/5, C/2, and C) for $Li_{1.3}V_3O_8$ | Li coin cells. (b) Capacity retention (values recorded in discharge) as a function of the number of cycles at different rates (C/10, C/5, and C) for $Li_{0.4}Cu_{0.9}V_3O_8$ | Li coin cells. Note that C/*n* corresponds to the total capacity discharged in *n* hours.

inserting up to 3.5 Li per formula unit (Figure 4b), and leading to capacities of 330 mAh/g were achieved. Although this ball milling process enhances the accessible capacity of the material, our composite electrode still suffers from a lack of conductivity at high current density, as conveyed by the evolution of the discharged capacity vs scan rate from C/1 up to C/10, Figure 5a. An increase in the discharge rate leads to a huge decrease in the capacity showing that our compound is strongly affected by kinetics. Less than 100 mAh/g is reversibly exchanged at a regime of C.

We believe that if Cu were extruded from $Li_{1.3-y}Cu_yV_3O_8$ the electrical conductivity of the electrode would be increased, and thus the rates might be higher. The voltage−composition traces for $Li_{0.4}Cu_{0.9}V_3O_8$/Li cell (Figure 4b) show that this material reversibly reacts with 3.3 Li per formula unit, leading to reversible capacities of about 260 mAh/g at C/8. The evolution of its discharged capacity vs. scan rate shows a capacity decrease of about 33% (Figure 5b) as the rate increases from C/10 to C. This contrasts with the 66% decrease, measured for the Cu-free LiV_3O_8/Li over the same rate window, suggesting a Li-driven Cu-extrusion mechanism process with $Li_{0.4}Cu_{0.9}V_3O_8$, so that the extruded copper most likely serves as an extra conducting additive. This improved rate capability does not translate into any noticeable advantage in terms of peak power/power rate over the Cu-free $Li_{1.3}V_3O_8$ phase owing to the lower initial capacities rooted in their heavier equivalent weight due to the substitution of Cu for Li.

Prolonged cycling indicates a better capacity retention for $Li_{1.3}V_3O_8$-based coin cells than for $Li_{0.4}Cu_{0.9}V_3O_8$-based ones. Indeed, for the former the capacity seems to stabilize at about 310 mAh/g after 100 cycles, whereas the capacity of the latter continuously and smoothly decreases from 275 to about 200 mAh/g over the first 100 cycles. The capacity retention of the Cu-free phase remains best for all cycling rates. The decline in reversibility as *y* increases in $Li_{1.3-y}Cu_yV_3O_8$ is a second hint that Cu does not fully participate in the Li-driven electrochemical redox process.

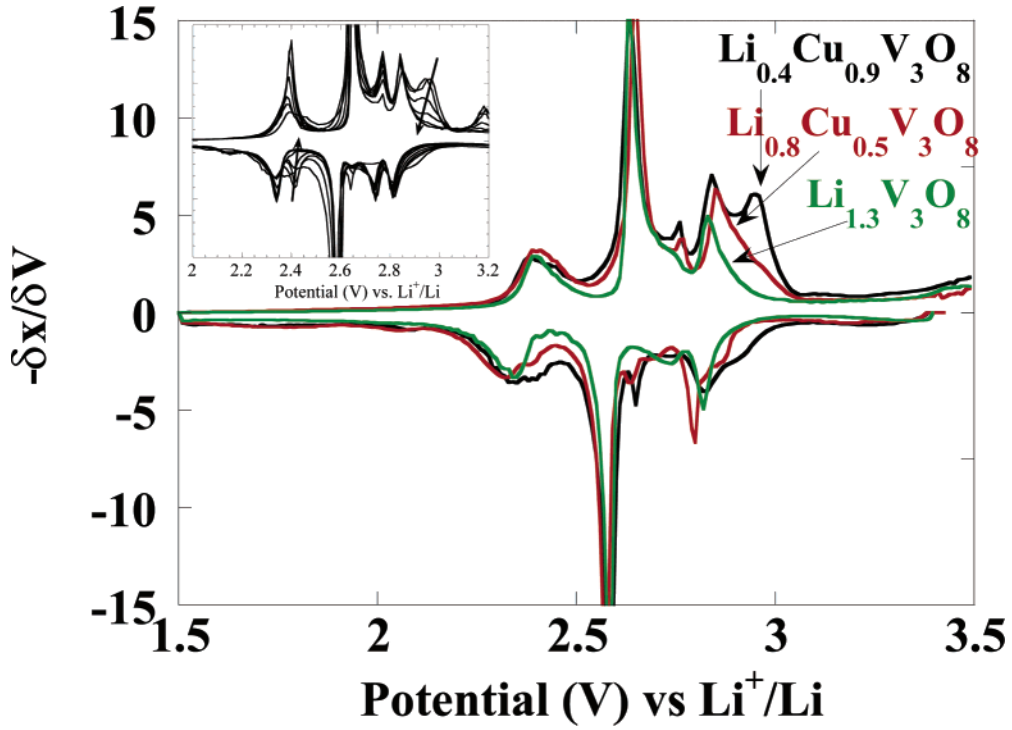

Figure 6. Evolution of the incremental capacity $\delta x/\delta E$ as a function of the potential during the intercalation/deintercalation process in $Li_{1.3}V_3O_8$, $Li_{0.8}Cu_{0.5}V_3O_8$, and $Li_{0.4}Cu_{0.9}V_3O_8$.

Finally, although the shape of the discharge/charge voltage curves for $Li_{0.4}Cu_{0.9}V_3O_8$-based cells is rather similar to that obtained for $Li_{1.3}V_3O_8$-based cells, there are small differences that can be observed on the incremental $\delta x/\delta V$ plots (Figure 6). A careful examination of these curves reveals a well-pronounced additional peak on oxidation located at 2.9 V and on reduction at 2.4 V. The intensity of these peaks is proportional to the amount of copper in the pristine material, and also decreases with cycling as shown in the inset, indicative that they are most likely associated with Cu extrusion/re-injection.

To check this hypothesis and gain further insight into the reaction of lithium with the $Li_{1.3-y}Cu_yV_3O_8$ system, a $Li_{0.4}Cu_{0.9}V_3O_8$/Li cell was assembled, and *in situ* X-ray measurements collected. The X-ray powder patterns collected during the cell discharge and charge (at C/40) and through subsequent cycles (Figure 7a) indicate the most relevant spectra, both as collected (bottom page) and as manipulated through pattern subtractions (Figure 7 caption), to concisely convey the fate of copper, without going into the details of phase transformations. On discharge, we observe Bragg peaks modifications (shifts/appearances/disappearances) that were used to delimit the three domains referred to as 1, 2, and 3 on the voltage composition curve (Figure 7a, top), and associated with a solid solution, biphasic, and solid solution domains, respectively. But more importantly, we note the appearance of a weak Bragg peak located at $2\theta = 43.2°$ attributed to Cu metal near $x = 1.2$, reaching maximum intensity at $x = 2$. This corresponds to the voltage plateau domain located at 2.57 V in the voltage composition curve that translates into the most intense peak in the derivative curve (Figure 7a, top right). On the basis of our previous study of $Cu_{2.33}V_4O_{11}$, the small amplitude of this Cu [111] peak suggests a limited Cu extrusion. On the subsequent charge, the overall process appears to be phase-wise reversible since again we found three-phase domains (denoted 4, 5, and 6) common with $Li_{1.3}V_3O_8$. Through this charging step, the copper peak remains constant in amplitude up to $x = 0.6$, and drastically decreases over the 2.9 V voltage plateau to become null for $x = 0$. We note that in domain 6 the copper metal peak remains unaffected, although the material has partially converted back into a $Li_xV_3O_8$-type structure. Because copper oxidation occurs at 3.4 V, we cannot eliminate the competing balance between simple copper oxidation and copper re-injection into the compound.

To check the extent of the Cu re-injection process and determine the texture and morphology of the extruded copper, we studied $Li_{0.4}Cu_{0.9}V_3O_8$ electrodes at various stages of the reduction processes by means of transmission electron microscopy (TEM). Here, we only report results for the precursor sample, the fully reduced electrodes (obtained after the first and 27th discharges), and finally the fully recharged (oxidized) electrode materials. The fresh electrode consists of 1000−2000-nm well-crystallized $Li_{0.4}Cu_{0.9}V_3O_8$ particles, as deduced from the diffraction pattern (Figure 8). For the fully reduced "$Li_{3.6}Cu_{0.9}V_3O_8$" the bright-field image (Figure 9a) indicates that it is mainly composed of a crystallized lithiated phase as deduced from the sharp spots displayed on the selected area electron diffraction (SAED) pattern

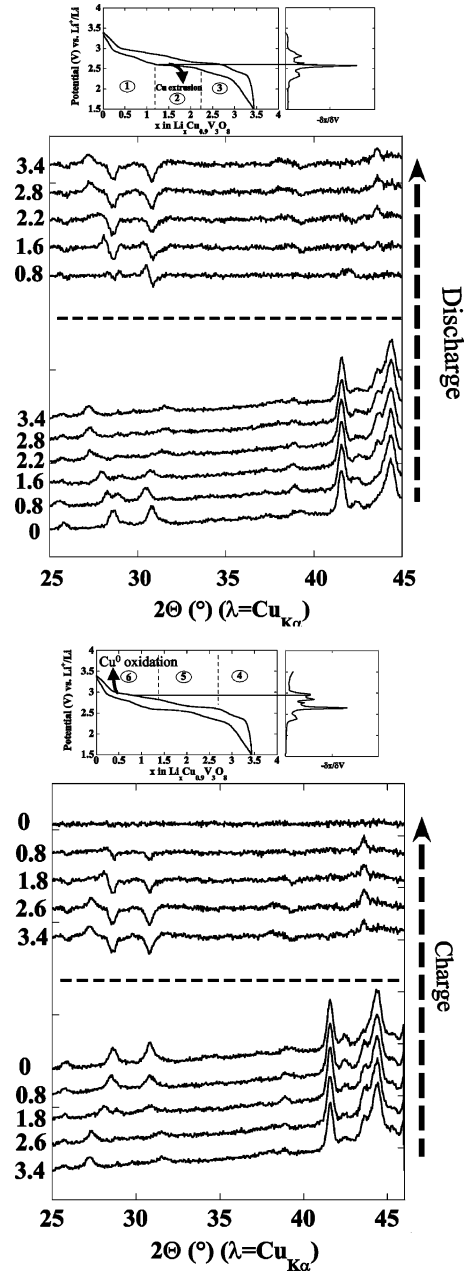

Figure 7. *In situ* X-ray diffraction recorded during the first discharge (a) of a $Li_{0.4}Cu_{0.9}V_3O_8$ | Li swagelok cell especially designed for that purpose. At the bottom of the figure specific diagrams were represented, and their difference with the initial diagram was plotted in the upper part of that figure. At the top, the different electrochemical processes emphasized by potentiodynamic. The same representation was used for the charge process (b).

(Figure 9a insert). The diffraction pattern may be indexed using the LiV_3O_8 structure type. Nevertheless, some extra spots are observed on the SAED pattern along the 001 direction mainly due to the presence of copper or imperfections as a result of the Li insertion/Cu extrusion process. With this phase we also notice a small amount of Cu nanoparticles having dimensions of about 20−30 nm (Figure 9b and c). The composition of this material determined by EDS is $Li_xCu_{0.8}V_3O_8$. The materials fully reduced after 13.5 cycles show a similar morphology but the amount of Cu nanoparticles has been increased (Figure 9d), and the amount of copper in the electrode material decreases, as deduced from the EDS measurements, to $Li_xCu_{0.4}V_3O_8$ (not shown

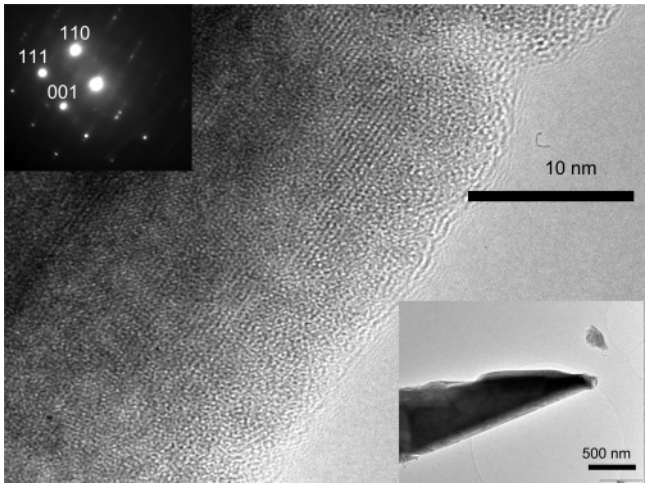

Figure 8. TEM study of the starting $Li_{0.4}Cu_{0.9}V_3O_8$ compound. The fresh electrode consists of well-crystallized 1000−2000-nm particles.

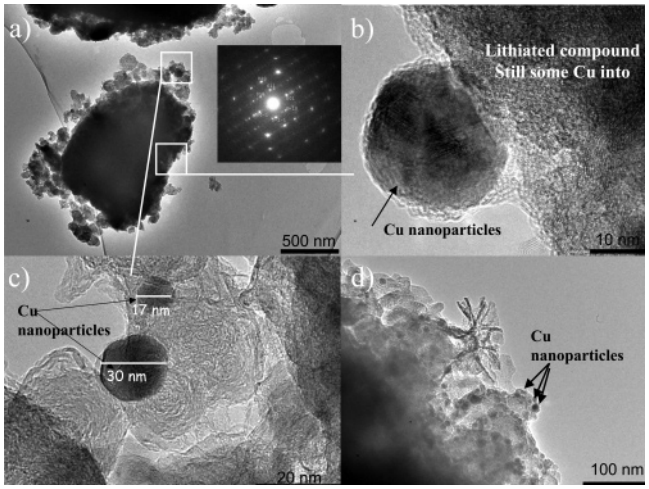

Figure 9. TEM study realized on the fully discharged $Li_{0.4}Cu_{0.9}V_3O_8$ electrode. (a) Overall bright-field image with SAED pattern indexed with $Li_{1.3}V_3O_8$-type phase, some extra spots along the c* axis were attributed to the presence of copper nanoparticles. (b−c) Zoom on one of these 30-nm nanoparticles. (d) After 13.5 cycles the Cu nanoparticles were again observed but the amount of copper hugely decreased as deduced from the global EDS measurements $Li_xCu_{0.4}V_3O_8$ composition.

here). Copper nanoparticles were also found to be present in the fully oxidized materials but in very small amounts on the edge of the particle (Figure 10). Furthermore, we also note that the copper distribution is heterogeneous with Li_x-$Cu_{0.4}V_3O_8$ on the edge and $Li_xCu_{0.9}V_3O_8$ at the particle core. In short, TEM measurements indicate that the morphology of the copper metal generated during the electrochemical insertion/deinsertion of Li in $Li_{1.3-y}Cu_yV_3O_8$ system and its outcome drastically differ from the Cu dendrites, previously observed on fully reduced "$Li_xCu_{2.33}V_4O_{11}$" composites, and then disappeared upon the subsequent charge.[12] Such partial irreversibility of the Cu extrusion/re-injection process is more likely responsible for the poor capacity retention of such compounds.

Discussion

Chemistry Route. It is well-known that only $Li_{1+x}V_3O_8$ samples with $x > 0$ can be prepared using solid-state routes.

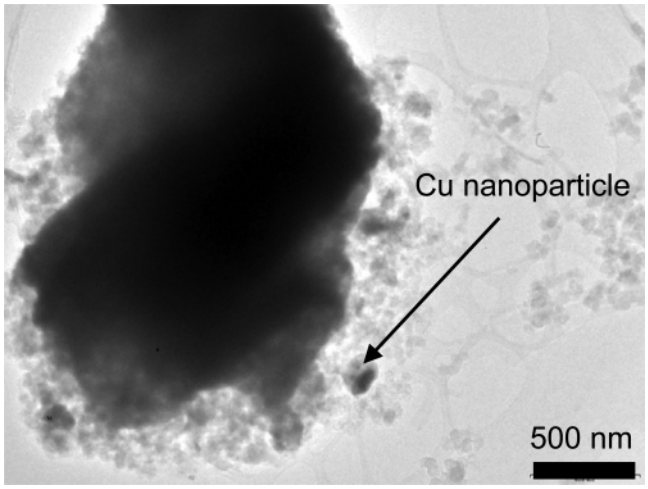

Figure 10. TEM study on the fully charged $Li_{0.4}Cu_{0.9}V_3O_8$ electrode. A few Cu nanoparticles can still be observed.

The desired stoichiometry is usually fixed to $x = 0.3$ or $x = 0.4$. Further lithiation by soft chemistry or electrochemistry routes allows, due to different thermodynamic conditions, a wider stoichiometry range in Li. This necessary lithium excess implies the presence of V^{4+} leading to the formula $Li_{1+x}V_{3-x}^{5+}V_x^{4+}O_8$.

A rational synthesis of any mixed valent metal oxide requires careful control of both cationic and oxygen stoichiometries. Even if the cationic portion is easy to control, the oxygen one depends on the reactants used as well as on the surrounding atmosphere. In principle, the oxygen stoichiometry is stable only in an atmosphere of appropriate and well-defined oxygen activity that is difficult to determine and master. Then, open tube methods can involve considerable empiricism. An alternative to control oxygen stoichiometry is the sealed tube approach. In this method, all of the elements need to be present in the desired stoichiometry (including oxygen). The oxygen pressure in the tube will "self-adjust" to that of the vapor pressure of the oxide(s) present.

This conclusion can be surprising if compared to the synthesis methods reported in the literature. $Li_{1+x}V_3O_8$ is usually made by heating in air a mixture of lithium-based reactant and V_2O_5, as reported by Wadsley et al. 50 years ago when, during his investigation of the binary diagrams $M_2O-V_2O_5$, he obtained a single crystal that, after a structural study, appeared to correspond to the compound $Li_{1.3}V_3O_8$.[1] But we believe it is a mistake to follow this "shake and bake" ceramic route to prepare pure $Li_{1.3}V_3O_8$ samples. This mistake is underlined, as reported in various papers, by the need to use lithium in excess and different heat treatments (close to the melting point) to stabilize the $Li_{1.3}V_3O_8$ phase. The key point to explain why nevertheless this procedure leads to obtaining the right compound is a well-known but difficult to master phenomenon, characteristic of some vanadates. Upon heating close to the melting point, some vanadates spontaneously liberate oxygen leading to an oxygen-deficient phase. It is the case, for example, for the silver vanadate $Ag_2V_4O_{11}$ that easily leads to the $Ag_2V_4O_{11-y}$ phase.[15] However, most of the time, there is an organization of the oxygen vacancies along crystallographic

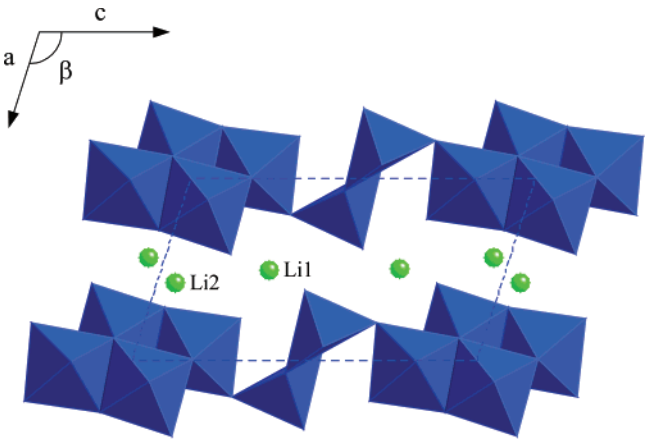

Figure 11. $Li_{1.3}V_3O_8$ projection onto the (010) plane.

directions or planes. To accommodate these extended defects, crystallographic shears appear leading to drastic structural changes occasionally resulting in the formation of a new compound. In the case of the silver-based vanadate this pseudo oxygen-deficient phase has actually been identified as corresponding to the $Ag_{1+x}V_3O_8$ phase.[16] The corresponding chemical equation can be written as follows:

$$\frac{3}{4}Ag_2V_4O_{11} \rightarrow \text{“}Ag_{1.5}V_3O_{8.25}\text{”} \rightarrow Ag_{1.5}V_3O_8 + \frac{1}{8}O_2\uparrow$$

By applying the same process to lithium-based vanadates, we could explain why $Li_{1.3}V_3O_8$ can be obtained even by heat treatment in air. Furthermore, in light of such considerations it is interesting to go back to Wadsley's paper to use his results to determine a better chemical route.

As explained above, $Li_{1.3}V_3O_8$ contains V^{4+} ions in an amount directly related to the lithium excess. Then one has to choose between two different routes. The first one is to use V^{5+}-based oxide and reductive lithium precursor. However, in this case it would be difficult to control the reduction process. The second is to directly use the appropriate amounts of V^{5+} and V^{4+}, meaning that the reaction will not enlist any internal reductive process. This also implies that the lithium precursor is "neutral" meaning that Li should be included in an oxide with one of the previous vanadium ions as described below.

$$(1+y)LiVO_3^{+} + (1-y)V_2O_5 + yVO_2 \rightarrow Li_{1+y}V_{3-y}^{5+}V_y^{4+}O_8$$

Indeed we have experienced that heating under vacuum a mixture of stoichiometric amounts of $LiVO_3$, VO_2, and V_2O_5 gives the desired phase in one step without any parasitic phases. Thus, following the same reasoning, the synthesis of $Li_{1.3-y}Cu_yV_3O_8$ solely implies the substitution of $y/2(Cu_2O, V_2O_5)$ for $yLiVO_3$ with the rest of the precursors remaining identical, in accordance with the process described in the Experimental Section.

$Li_{1.3-y}Cu_yV_3O_8$ Solid Solution. At this point, a legitimate question deals with the nonexistence of a complete $Li_{1.3-y}Cu_yV_3O_8$ solid solution. An examination of the $Li_{1.3}V_3O_8$ structure (Figure 11) can give clues to understanding why this solid-state homogeneity range does not exceed $y = 1$. The structure is built up of $[V_3O_8]$ layers developed in the **b**−**c** plane, and stacked along the **a** axis. Li cations ensure the cohesion of the layers. The Li are localized in two independent crystallographic sites. The principal one corresponds to an octahedral-oxygenated surrounding, and when fully occupied it gives the composition $Li_1V_3O_8$. The extra 0.3 lithium is localized in a partially occupied second crystallographic site that corresponds to a tetrahedral-oxygenated surrounding. For $Li_{1.3-y}Cu_yV_3O_8$ the upper limit of the solid solution being $y = 1$, we conclude that the copper ions are inserted in the first and fully occupied site only.

Then the problem is to understand why the second site cannot be occupied by copper ions. For $y = 0$ ($Li_{1.3}V_3O_8$), such a site corresponds to a tetrahedral surrounding that can be adopted by copper ions. However, examination of the cell parameters evolution (Table 1) shows that, even if the layers remain unchanged (**b** and **c** cell parameters constant), the layer packing is affected by the presence of copper. This can be ascribed to a gliding of the layers necessary to accommodate the copper environment in the main site, which also affects the second site becoming incompatible for copper ions. Then, it appears reasonable to say that, only lithium can fit this second site, and that its presence is necessary to stabilize the structure, explaining why all attempts at preparing $Cu_{1+x}V_3O_8$ samples have failed.

Despite different synthesis routes, for y greater than 1, the samples were multiphased with $\beta Cu_xV_2O_5$ as the main impurity phase. Such a finding can also be related to the spontaneous above-mentioned loss of oxygen, according to the following chemical equation: $^2/_3Cu_{1+x}V_3O_8 \rightarrow$ "$Cu_yV_2O_{5.33}$" $\rightarrow Cu_yV_2O_5 + {}^1/_6\,6O_2\uparrow$. Here again, as the synthesis is done under vacuum, we can suspect that if the $Cu_{1+x}V_3O_8$ compound is formed, it is not stable, and transforms into the $Cu_xV_2O_5$ phases. At this point, it is also interesting to compare the relative stability of the obtained phases using Li, Ag, or Cu. In the case of Li, even in air, it is possible to stabilize the $Li_{1.3}V_3O_8$ compound while "$Li_2V_4O_{11}$" has never been reported. Using Ag, both $Ag_{1.3}V_3O_8$ and $Ag_2V_4O_{11}$ can be isolated but the heating of $Ag_2V_4O_{11}$ easily leads, through the spontaneous loss of oxygen, to the $Ag_{1.3}V_3O_8$ phase. With copper, only $Cu_{2.33}V_4O_{11}$ has been reported, while all attempts at preparing the $Cu_{1.3}V_3O_8$ phase have led to stable copper vanadates or copper vanadium bronzes, whatever the synthesis routes and copper precursors used. Moreover, heating under vacuum all these oxides led to the same $M_xV_2O_5$ phases in different ratios to balance the M cation content.

Finally, the difficulty in preparing pure $Cu_{1.3}V_3O_8$ sample may also be nested in the specific behavior of copper and vanadium during synthesis. In the case of lithium and silver, the valence state +I is maintained, and no internal oxidation−reduction process occurs. Appropriate amounts of each of the reactants and of their respective valence state are preserved in the final product. In the case of copper, we carried out the synthesis using Cu^{1+}, and applied the chemical reaction elaborated for lithium-based compounds. However, for $y > 1$, the internal redox reaction $Cu^{1+} + V^{5+} \rightarrow Cu^{2+} + V^{4+}$, which we previously ruled out based on both magnetic and EPR measurements for $y < 1$, could occur.

(16) Raveau, B. *Rev. Chim. Miner.* **1967**, *4*, 729.

This implies that when using copper not only the nature and amount of inserted cations are modified but also the V^{4+}/V^{5+} ratio, so that the amount of V^{4+} might be too high to allow such a phase to be stable (for $y > 1$) via high-temperature solid-state routes. Hence the existence of a delicate balance between the two Cu^{1+}/Cu^{2+} and V^{4+}/V^{5+} redox centers.

Returning to the electrochemistry of $(Li_{1.3-y}Cu_y)V_3O_8$, explanations are needed regarding (1) the excellent cyclability of the Cu-free sample ($y = 0$) synthesized in a one-step sample and (2) the limited Cu extrusion−re-injection in an apparently quite flexible structure.

There has been a tremendous amount of data reporting the interplay between the synthesis conditions of $Li_{1.3}V_3O_8$ powders and their electrochemical performances. Numerous claims have been made on the importance of particle morphology, texture, size, or even residual water to achieve good capacity retention. In comparison to the previous sol−gel or ceramic methods, although costly, our sealed ampule process provides a nice way to obtain materials free from traces of water, and enables stoichiometry control, thereby mastering the delicate balance between oxygen stoichiometry and the V^{+4}/V^{+5} ratio for optimum phase purity. Such purity can be reached by the ceramic processes, but requires several annealing/grinding steps.

The different electrochemical behavior of $(Li_{1.3-y}Cu_y)V_3O_8$ compared to that of $Cu_{2.33}V_4O_{11}$ comes at first as a surprise. Not only are a different Cu morphology and a limited Cu extrusion process found, but also a poor reversibility of the extruded copper. This was surprising since a greater flexibility of the V−O layers was expected for the $(Li_{1.3-y}Cu_y)V_3O_8$ phases owing to the presence of two pivot oxygens. This simply means that structural flexibility is a necessary, but certainly not a sufficient, parameter to explain Cu displacement reactions. Other criteria, such as high ionic Cu diffusion and suitable redox energy levels are necessary. Obviously there is a drastic difference between the crystallographic sites occupied by Cu in the two structures, namely with Cu^+ ions highly delocalized over trigonal/linear sites within the $Cu_{2.33}V_4O_{11}$ phase as compared to well localized (e.g., tetrahedral sites) for the $(Li_{1.3-y}Cu_y)V_3O_8$ structure. Could such a difference be sufficient to explain the various Li reactivity pathways? This remains an open question. We also cannot fail to mention the competition between the Cu^{1+}/Cu and V^{+5}/V^{+4} redox levels (i.e., the respective position of the Cu^+ to V^{+5} acceptor energy levels). To further exploit this argument quantitatively will require electronic structure calculations currently in progress. Finally, regarding the growth of copper nanoparticles vs dendrites, we believe that it is not related to structural differences between the host materials, but more to current density issues, since we have recently shown, studying the Li electrochemical reduction of $Cu_{2.33}V_4O_{11}$, that high current densities can lead to copper nanoparticles as compared to submicron dendrites for low current densities.[17]

Conclusions

We have reported the synthesis of $(Li_{1.3-y}Cu_y)V_3O_8$ solid solution for $0 < y < 1$ based on a one-step process. The rationale is explained in terms of stoichiometry control, charge neutrality arguments, and structural considerations. The electrochemical performance of such materials, namely in terms of capacity and cycle life, were shown to be worse than those of the end member phase $y = 0$. Their reactivity toward Li revealed the competition between the classical insertion/deinsertion process and the recently reported Cu extrusion/re-injection process with the former being, by far, dominant. Through this study we have further stressed the complex chemistry of such Cu-based vanadates rooted in their various redox couples, and also the difficulty in identifying materials that, like $Cu_{2.33}V_4O_{11}$, can react with Li through a fully reversible Cu extrusion/re-injection process. It becomes apparent that, besides the high structural flexibility, the structural localization/delocalization of the copper ions and, more importantly, the relative position of Cu^{1+} vs V^{5+} acceptor energy levels are of tremendous importance. In the absence of electronic structure calculations, we simply proceed by trial and error in the search for suitable materials able to undergo Li-driven displacement reactions. Such a search is not presently limited to Cu-based vanadates but also extended to Ag-based ones that, in light of the above criteria, could be prone to such types of reactions.

Acknowledgment. We are indebted to J. Galy's willingness to share with us his long experience on vanadates and D. W. Murphy for enlightening discussions.

CM048518F

(17) Rozier, P.; Galy, J. *J. Solid State Chem.* **1997**, *134*, 294.
(18) Poizot, P.; Chevallier, F.; Laffont, L.; Morcrette, M.; Rozier, P.; Tarascon, J−M. *J. Electrochem. Solid State Lett.*, in press.